Precambrian Research 378 (2022) 106749

Contents lists available at ScienceDirect

Precambrian Research

journal homepage: www.elsevier.com/locate/precamres

Mercury isotopes reflect variable metal sources as a function of paleo-depositional setting in the Ediacaran-Cambrian Ocean, South China

Zhongxi Xue [a,b], Runsheng Yin [c,*], Bernd Lehmann [d], Ruidong Yang [a,b], Hai Xu [a,b], Jun Chen [a,b], Hongyan Geng [e], Junbo Gao [a,b,*]

[a] College of Resources and Environmental Engineering, Guizhou University, Guiyang 550025, China
[b] Key Laboratory of Karst Georesources and Environment, Ministry of Education, Guizhou University, Guiyang 550025, China
[c] State Key Laboratory of Ore Deposit Geochemistry, Institute of Geochemistry, Chinese Academy of Sciences, Guiyang 550081, China
[d] Mineral Resources, Technical University of Clausthal, Clausthal-Zellerfeld 38678, Germany
[e] Science Unit, Lingnan University, Hong Kong

ARTICLE INFO

Keywords:
Hyperenriched metalliferous black shale
Early Cambrian
Seawater
Oceanic anoxic event
Mercury
Hg isotopes

ABSTRACT

A broad spectrum of marine sediments, including metalliferous black shales, stratiform barite, phosphorite and sapropelite (combustible shale) was widely deposited during the Ediacaran-Cambrian transition on the Yangtze Platform. The source of metals in the metalliferous black shales and the trigger for ocean dynamics during this critical period remain controversial. We analyzed Hg isotopes in late Ediacaran to Early Cambrian carbonaceous sedimentary rocks from the basinal Sansui section, South China, and observed Hg concentrations of 10^2–10^3 ppb, which is high but within the global range of black shales. The late Ediacaran carbonaceous chert shows near-zero Δ^{199}Hg values (−0.05–0.09‰), which can be interpreted as input of terrestrial Hg or volcanic Hg. However, the transgressive near-coastal setting supports the terrestrial origin. The Early Cambrian V rich black shales display positive Δ^{199}Hg values (0.03–0.18‰), which are similar to those observed in polymetallic Ni-Mo-rich sulfidic black shales (0.10–0.22‰) and phosphorites (0.13–0.24‰) in the stratigraphically equivalent Maoshi and Zhijin sections, respectively. These positive Δ^{199}Hg values suggest that Hg was of dominantly seawater origin in a restricted basin setting. The variable Δ^{199}Hg values of the rock spectrum reflect the dynamic interplay of marine and terrestrial metal sources as a function of paleo-depositional setting within the transgressive–regressive system on the continental margin of the Ediacaran-Cambrian Yangtze platform.

1. Introduction

The Ediacaran-Cambrian (E-C) transition is a critical period for the rise of atmospheric/oceanic oxygen levels and the development of most phyla of modern animals and modern-like marine ecosystems (Li et al., 2017; Darroch et al., 2018; Wood et al., 2019). The plate rearrangement from the Rodinia to the Gondwana supercontinent was accompanied by large-scale continental flooding and rapid continental motion with peak true polar wander at ca. 525 Ma which induced transgressive events with an unusual micro-environmental spectrum (Kirschvink et al., 1997; Mitchell et al., 2015). The rifted continental margin of the Yangtze platform in South China displays a sequence of Early Cambrian black shale which hosts stratiform barite and manganese deposits, phosphorite, combustible sapropelite (“stone coal”), vanadium-rich shale, and locally hyperenriched metalliferous black shale units (Mo-Ni-rich sulfide units) (Coveney et al., 1994; Steiner et al., 2001). The sources of metals in these deposits and metalliferous shale have been explained by two opposite models: (1) submarine hydrothermal venting (Lott et al., 1999; Steiner et al., 2001; Jiang et al., 2006; Han et al., 2015, 2017; Zhou et al., 2018; Zhu et al., 2021a) and (2) scavenging from seawater in redox-stratified basins (Mao et al., 2002; Lehmann et al., 2007; Xu et al., 2011, 2013; Xu and Mao, 2021; Yin et al., 2017). These models have different implications on ocean dynamics and metal cycling, and can be re-evaluated by using mercury (Hg) isotope systematics.

Mercury (Hg) is enriched in the Early Cambrian sulfide- and Mo-Ni-rich black shale units together with a broad spectrum of redox-sensitive chalcophile metals (Lehmann et al., 2007; Yin et al., 2017; Zhu et al., 2021b). Euxinic depositional environments, such as marine black shale,

* Corresponding authors at: State Key Laboratory of Ore Deposit Geochemistry, Institute of Geochemistry, Chinese Academy of Sciences, Guiyang 550081, China (R. Yin) and College of Resources and Environmental Engineering, Guizhou University, Guiyang 550025, China (J. Gao).
E-mail addresses: yinrunsheng@mail.gyig.ac.cn (R. Yin), jbgao@gzu.edu.cn (J. Gao).

https://doi.org/10.1016/j.precamres.2022.106749
Received 19 February 2022; Received in revised form 15 May 2022; Accepted 21 May 2022
Available online 4 June 2022

can have elevated Hg contents with a global mean of 320 ppb Hg (Ketris and Yudovich, 2009), compared to average shale with 64 ppb Hg (Grasby et al., 2019) and the average continental crust with about 30 ppb Hg (Rudnick and Gao, 2003). As a volatile metal, Hg is emitted primarily from volcanic activities (Grasby et al., 2019) and can undergo global transport in the atmosphere prior to deposition into terrestrial and oceanic ecosystems (Selin, 2009). In the ocean, Hg can be scavenged from seawater via the organic matter shuttle and buried into sediments (Yin et al., 2017). Mercury stable isotopes (196, 198, 199, 200, 201, 202 and 204, amu), which undergo mass-dependent fractionation (MDF, usually defined as δ^{202}Hg) and unique mass-independent fractionation (MIF, usually defined as Δ^{199}Hg), can provide critical information on the Hg cycle (Blum et al., 2014). In particular, Hg-MIF, which occurs mainly via photochemical processes with little contribution from other reactions, can provide clear source constraints (Blum et al., 2014; Kwon et al., 2020). Volcanic Hg derived from the primitive mantle has limited Hg-MIF signals (Δ^{199}Hg ~ 0; Zambardi et al., 2009; Moynier et al., 2021; Yin et al., 2022). However, Hg(II) photoreduction processes on Earth's surface result in negative Δ^{199}Hg in terrestrial materials (e.g., soil and vegetation) and positive Δ^{199}Hg in marine materials (e.g., seawater and marine sediments) (Blum et al., 2014). Given these diagnostic features, Hg-MIF may help to constrain the source of Hg in the enriched Early Cambrian rock units, such as terrestrial, seawater and volcanic sources.

A recent study on two Early Cambrian shale sections of the Niutitang Formation of South China (Maoshi and Zhijin sections) has shown overall positive Δ^{199}Hg values in both phosphorite and Ni-Mo-rich polymetallic sulfidic shale, suggesting that Hg was sourced from seawater (Yin et al., 2017). We here add additional data from the Sansui section at the Bagong vanadium deposit, which covers the latest Ediacaran Liuchapo Formation and overlying Early Cambrian lower Jiumenchong Formation, and provides a broader view at the E-C transition on the Yangtze Platform. Our data suggest significant changes in metal sources as a function of near-coastal versus restricted basin setting.

2. Geological background

During the E-C transition, South China, consisting of the Yangtze platform and Cathaysia Block (Fig. 1), was under a low paleo-latitude and in a passive margin setting (Zhu et al. 2003; Merdith et al., 2021). Sedimentation in the Yangtze Platform has been paleogeographically recognized as shallow shelf facies (carbonate platform) in the northwest to transitional and deep basinal facies of black shale and chert in the southeast (Zhu et al., 2003; Wallis, 2007). Segmented carbonate uplifts separated the transitional zone from the deep basin, forming a locally restricted offshore basin environment at the transition zone (Zhu et al., 2003). Polymetallic sulfide-rich shale (e.g., Ni-Mo-V-Ba-PGE) and phosphorite units occur discontinuously over a strike length of >1500 km in the basal Early Cambrian Niutitang Formation (and equivalent formations). The polymetallic Ni-Mo-sulfide-rich shale is in the restricted offshore basin facies, whereas the phosphorite deposits occur both in the restricted offshore basin facies and the relatively shallower carbonate platform margin facies (Fig. 1).

The studied Sansui section in eastern Guizhou (N: 26°95′, E: 108°67′), and the two previously studied Maoshi (N: 27°49′, E: 106°46′) and Zhijin (N: 26°35′, E: 105°52′) sections in northern and western Guizhou, respectively, are located in the restricted offshore basin facies. As shown in Fig. 2, the Maoshi and Zhijin sections comprise the late Ediacaran Dengying Formation (dolomite), and the overlying Early Cambrian Niutitang Formation (black shale), separated by a disconformable erosional contact with karst features. A 10 cm-thick polymetallic sulfide-rich black shale unit and a stratigraphically equivalent up to 20 m-thick lower unit of phosphorite are hosted in the basal Niutitang Formation at Maoshi and Zhijin, respectively (Yin et al., 2017). The Sansui section (Fig. 2) comprises the late Ediacaran Liuchapo Formation (carbonaceous chert, equivalent to the Dengying Formation) and the Early Cambrian Jiumenchong Formation (black shale, equivalent to the Niutitang Formation). Different from the Maoshi and Zhijin sections, no unconformity or stratigraphic hiatus was observed between the two formations at Sansui (Chen et al., 2015). The upper part of the Liuchapo Formation hosts two tuff units (bentonite) which gave CA-ID-TIMS U-Pb concordia ages on zircon of 536.6 ± 0.7 Ma (1.2 m below the contact of the Liuchapo and Niutitang Formations) and 541.5 ± 0.4 Ma (2.4 m below the contact of the Liuchapo and Niutitang Formations) (Wang et al., 2020). A 50-cm-thick polymetallic V-rich unit, consisting of black shale and carbonaceous chert with dolostone lenses and phosphorite nodules, is observed in the basal Jiumenchong Formation, which is stratigraphically comparable with the Ni-Mo layer in the Maoshi section and the phosphorite deposit in the Zhijin section in the Niutitang Formation. A recent study yielded a LA-ICPMS U-Pb concordia age on zircon of 520.9 ± 1.0 Ma for a tuff layer in the polymetallic V-rich unit at Sansui (Wu et al., 2021), which is similar to the zircon U-Pb age for the phosphorite deposit at Zhijin (522.7 ± 4.9 Ma; Wang et al., 2012) and the Re-Os age for the polymetallic Ni-Mo-rich layer at various mine sites in Guizhou and Yunan (521.0 ± 5.0 Ma; Xu et al., 2011) (Fig. 2). Unlike

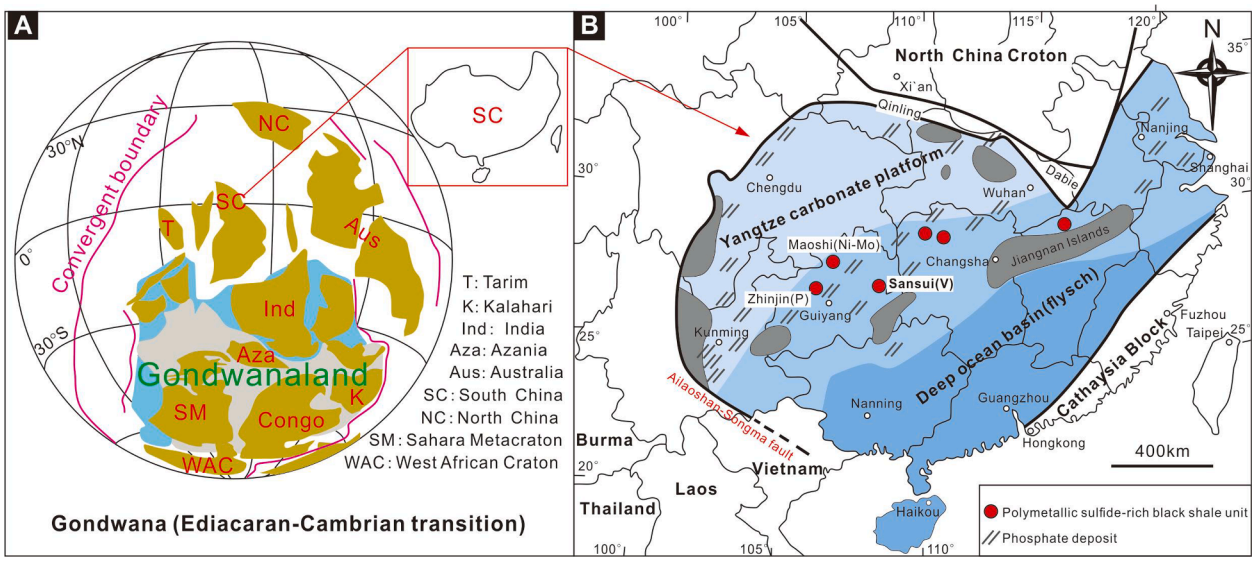

Fig. 1. (A) Paleo-plate tectonic model during the E-C transition (modified from Merdith et al. 2021). (B) Simplified map showing the paleogeography of the Yangtze Platform during the E-C transition (modified from Lehmann et al., 2016).

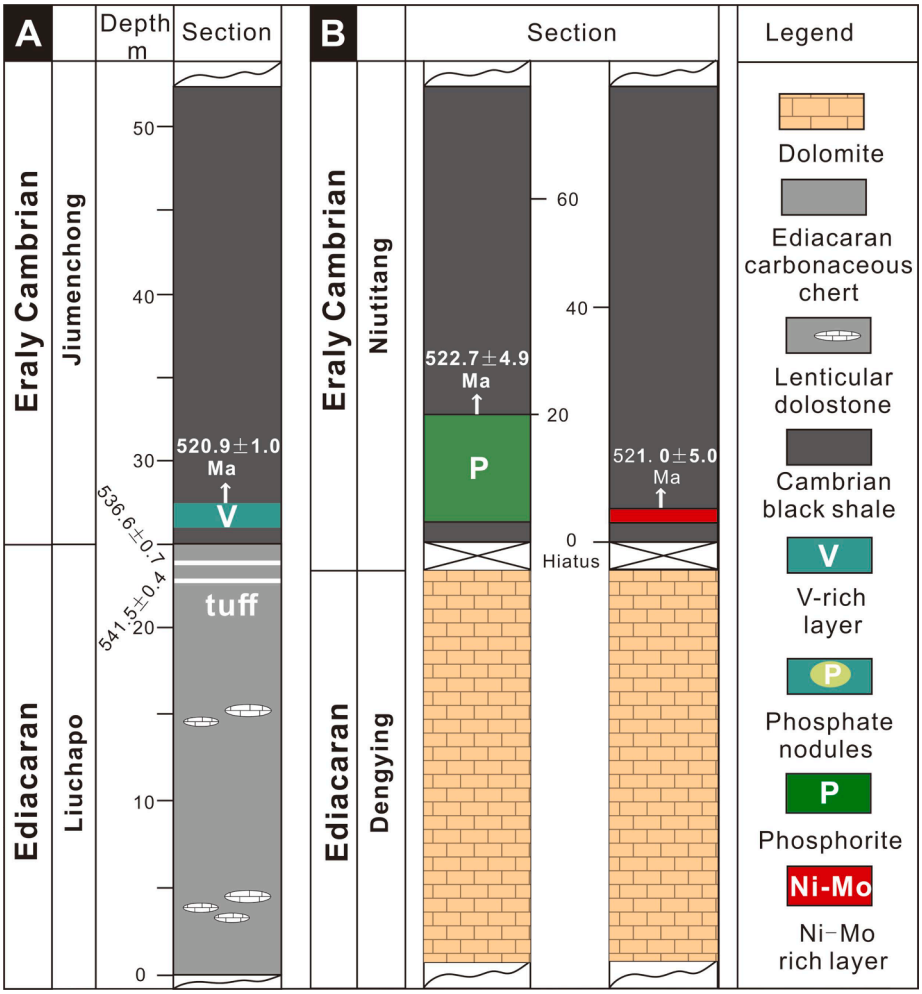

Fig. 2. Stratigraphic columns showing the E-C sedimentary sequences of (A) the Sansui section and (B) the Zhijin and Maoshi sections (modified from Yin et al., 2017).

the Maoshi and Zhijin sections, a paleo-uplift area is closely located near the Sansui section, which is part of the Jiangnan paleo-islands (Fig. 1**B**).

3. Methods

3.1. Sample collection and preparation

Bulk rock samples (n = 19) were collected from the Sansui section over a stratigraphic interval of 26 m, including 11 samples (carbonaceous chert and dolostone) from the Liuchapo Formation and 8 samples (black shale) from the Jiumenchong Formation (Fig. 2**A** and **Table S1**). The samples from the Jiumenchong Formation include an 0.5-m-thick interval of V-rich black shale which is mined for vanadium. After carefully removing all weathered surfaces, the samples were cleaned, dried, powdered to 200 mesh size and homogenized, prior to chemical analysis.

3.2. Hg concentration and isotopic composition analysis

Total Hg concentrations were measured by a Milestone DMA-80 atomic absorption spectrophotometer, which yielded Hg recoveries of 90–100% for the soil reference material SRM GSS-5. The relative standard deviations of Hg concentrations for replicate samples were all < 10%. A double-stage tube furnace was used to preconcentrate Hg from the samples into 5 mL of 40% acid mixture (HNO_3/HCl = 3/1, v/v) (Zerkle et al., 2020). The preconcentrated Hg was then analyzed by Neptune Plus multi-collector inductively coupled plasma mass spectrometry at the Institute of Geochemistry, Chinese Academy of Sciences (IGCAS), following the method described in Yin et al. (2016). Hg-MDF is expressed in δ^{202}Hg notation in units of permil (‰) referenced to the NIST-3133 Hg standard (analyzed before and after each sample analysis):

$$\delta^{202}Hg(‰) = \left[\left(^{202}Hg/^{198}Hg_{sample}\right)/\left(^{202}Hg/^{198}Hg_{standard}\right) - 1\right] \times 1000$$

Hg-MIF is reported in Δ notation, which describes the difference between the measured δ^{xxx}Hg and the theoretically predicted δ^{xxx}Hg value, in units of ‰, with xxx = 199, 200 or 201:

$$\Delta^{xxx}Hg \approx \delta^{xxx}Hg - \delta^{202}Hg \times \beta$$

β is equal to 0.2520 for ^{199}Hg, 0.5024 for ^{200}Hg, and 0.7520 for ^{201}Hg (Blum and Bergquist, 2007). The Hg concentration and acid matrices of NIST-3133 standard solutions were matched with the sample solutions. Long-term analytical uncertainties were assessed by replicate analyses of NIST-3177 secondary standard solutions, which yielded δ^{202}Hg of −0.53 ± 0.11‰, Δ^{199}Hg of −0.02 ± 0.06‰, Δ^{200}Hg of 0.01 ± 0.05‰ and Δ^{201}Hg of −0.01 ± 0.07‰ (2σ, n = 4). Soil standard reference material GSS-4 was prepared the same way as the samples and yielded δ^{202}Hg of −1.71 ± 0.12‰, Δ^{199}Hg of −0.38 ± 0.07‰, Δ^{200}Hg of 0.01 ± 0.06‰ and Δ^{201}Hg of −0.39 ± 0.07‰ (2σ, n = 3). The larger values of standard deviation (2σ) for either NIST-3177 or GSS-5 are used to reflect analytical uncertainties.

3.3. Total organic carbon and trace element analysis

Major elements and total organic carbon (TOC) were measured at the ALS Chemex (Guangzhou) Co. Ltd. by a Philips PW2424 X-ray fluorescence spectrometer (XRF) and Leco CS230 carbon/sulfur analyzer. Trace elements were measured at IGCAS by inductively coupled plasma mass spectrometer (ICP-MS) with a PerkinElmer ELAN DRC-e quadrupole (Q-ICP-MS), following a method reported previously (Han et al., 2018). The analytical accuracy was better than 5% for the measured elements. Al-normalized enrichment factors (EF) of Mo and U are proxies of oceanic redox conditions, which were calculated by the equation $X_{EF} = [(X/Al)_{sample}/(X/Al)_{AUC}]$ (Tribovillard et al., 2006, 2012; Algeo and Tribovillard, 2009), where X represents Mo or U, and AUC represents average upper continental crust. The AUC data were taken from McLennan (2001).

4. Results

The analytical data are compiled in **Table 1**, and some parameters are graphically shown in Fig. 3. Samples of the late Ediacaran Liuchapo Formation have 1.5 ± 1.2 wt% Al_2O_3 (1 SD; n = 11) and 2.2 ± 1.0 wt% C_{org} (1 SD; n = 8), with the three samples from dolostone lenses excluded. This is different from the black shale and siliceous black shale samples of the Early Cambrian Jiumenchong Formation with 11.8 ± 7.1 wt% Al_2O_3 (1 SD; n = 8) and 5.5 ± 4.7 wt% C_{org} (1 SD; n = 8), respectively. A sample in the Liuchapo Formation (SYC-08) shows visible barite and extremely high Ba concentration (82,100 ppm). The Jiumenchong Formation samples are enriched in redox-sensitive elements such as V (609–7830 ppm), Cr (124–748 ppm), Mo (12.8–89.3 ppm), U (10.4–125 ppm) and Hg (287–4260 ppb), and positive correlations can be observed between V and Cr, Mo, U and Hg in these samples (Fig. 4).

Yin et al. (2017) also reported very high Hg concentrations in the Early Cambrian polymetallic Ni-Mo layer (Hg: 15800 ± 6960 ppb, SD; and elevated TOC: 21.9 ± 1.98 wt%, 1 SD) and in phosphorites (Hg: 1030 ± 892 ppb, SD; TOC: 1.30 ± 0.85 wt%, 1 SD) from the Maoshi and Zhijin sections, respectively. The Liuchapo Formation displays average δ^{202}Hg of −0.07 ± 0.56‰ (1 SD) and average Δ^{199}Hg of 0.01 ± 0.04 ‰ (1 SD), while the Jiumenchong Formation displays average δ^{202}Hg of 0.14 ± 0.14‰ (1 SD) and average Δ^{199}Hg of 0.04 ± 0.08 ‰ (1 SD). Two samples from the polymetallic V unit show distinctly positive Δ^{199}Hg values (SYC-18: 0.12‰; SYC-19: 0.18‰), which are similar to those observed in polymetallic Ni-Mo-rich sulfidic black shales (0.10–0.22‰) and phosphorites (0.13–0.24‰) from the Maoshi and Zhijin sections, respectively (Yin et al. 2017).

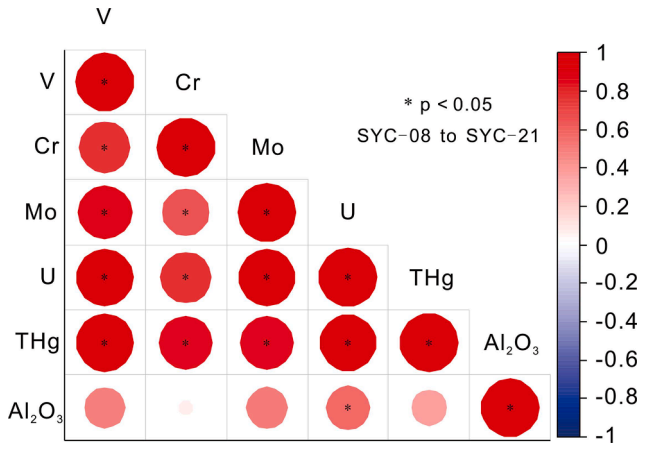

Fig. 4. Correlation diagram between V and Cr, Mo, U, Hg, Al_2O_3 for the upper 15 m of the sample section (SYC-08 to SYC-21). Size of circles and intensity of color shading refer to the strength of correlation.

5. Discussion

5.1. Changes in depositional environment and oceanic redox conditions during the E-C transition

Mo/TOC ratios reflect the degree of restriction in marine environments, with values of >35 ppm/%, 15–35 ppm/%, and <15 ppm/% relating to weak, moderate, and strong restriction, respectively (Algeo and Lyons, 2006). The Sansui samples show Mo/TOC ratios of 6.6 ± 4.8 (Fig. 5**A**), reflecting basin conditions of strong restriction during the E-C transition. A restricted environment in the offshore basins at the transition zone of the Yangtze platform is documented by the very variable thickness of the Niutitang Formation (Zhu et al., 2003). Segmented carbonate uplifts separated the transitional zone from the deep basin (Fig. 1**B**), which may have played an important role in forming a restricted offshore basin environment at the transition zone.

The Mo_{EF} versus U_{EF} diagram (Fig. 5**B**) suggests a redox fluctuation in the depositional environments at the E-C boundary. The Mo_{EF} and U_{EF} values of the lowermost part of the section (0–7.5 m with values of < 10) suggest suboxic conditions, also seen in the lowermost 0.2 m of the Jiumenchong Formation, whereas the much higher Mo_{EF} and U_{EF} values

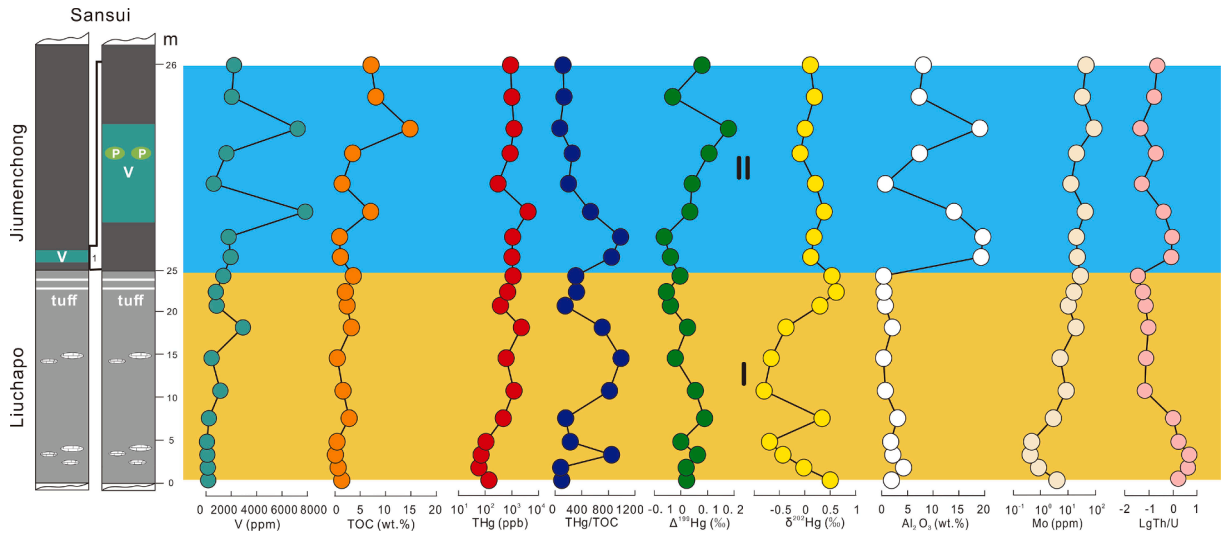

Fig. 3. Stratigraphic distribution of TOC, THg, THg/TOC ratio, Δ^{199}Hg, δ^{202}Hg, Al_2O_3, Mo and CIA for the Sansui section samples.

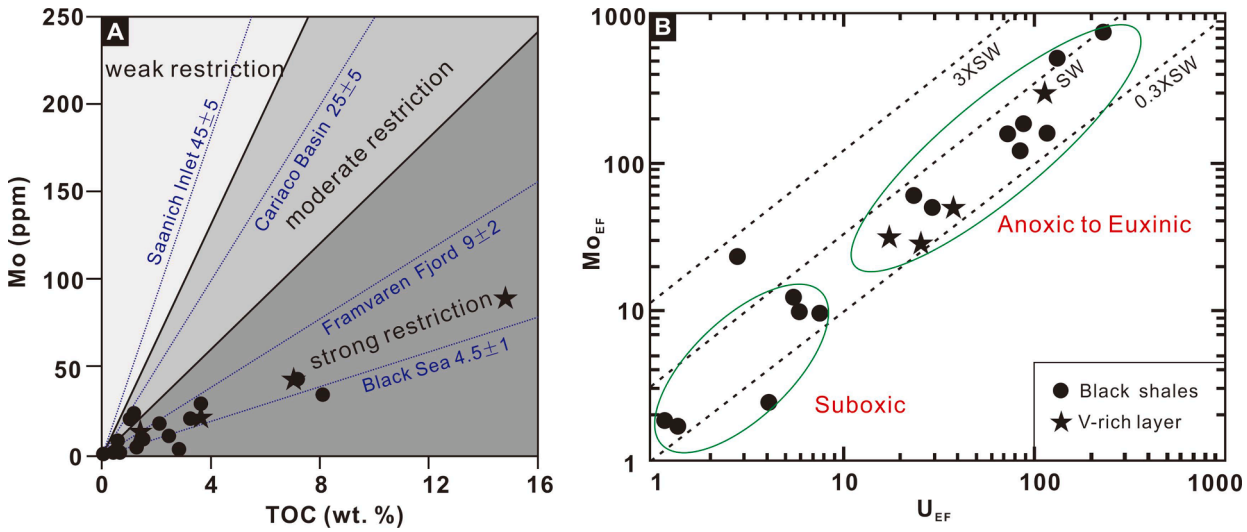

Fig. 5. (A) Mo versus TOC (modified from Algeo and Lyons, 2006) and (B) Mo_{EF} versus U_{EF} for the Sansui section samples.

in the upper part of the Liuchapo Formation and the V-rich unit of the Jiumenchong Formation and above suggest anoxic and possibly up to euxinic conditions (Li et al., 2010, 2017; Fan et al., 2018; Qin et al., 2022), which can be supported by Th/U index as well (Fig. 3).

5.2. *Changes in Hg sources to the ocean during the E-C transition*

Samples in this study show Hg concentrations (10^2–10^3 ppb) similar or higher compared to those observed in average marine black shale (320 ppb Hg, Ketris and Yudovich, 2009), and much higher than the average shale value of Hg of 64 ppb (Grasby et al., 2019). Hg isotopes (especially Δ^{199}Hg) can trace the source of Hg, since volcanic Hg has Δ^{199}Hg of ~ 0, while terrestrial reservoirs (e.g., soil) have negative Δ^{199}Hg values and marine reservoirs (e.g., seawater) have positive Δ^{199}Hg values (Blum et al., 2014). The variation of Δ^{199}Hg observed in our study suggests subtle changes in Hg sources in the ocean, during the E-C transition.

The late Ediacaran carbonaceous chert in the Sansui section shows Δ^{199}Hg values close to zero (−0.05–0.09 ‰), which could be explained by input of volcanic Hg with near-zero Δ^{199}Hg values (Zambardi et al., 2009). The break-up of Rodinia associated with volcanism, and the Central Iapetus magmatic province (CIMP), may explain the generally high Hg concentrations and the near-zero Δ^{199}Hg values in the Ediacaran carbonaceous chert, consistent with the interpretation of Hg data on marine sediments and related LIP events at other geologic times (Grasby et al., 2019). Alternatively, the near-zero Δ^{199}Hg values can also be explained as input of terrestrial Hg with negative Δ^{199}Hg values. Plants transfer atmospheric Hg(0) into the soil, resulting in negative Δ^{199}Hg in terrestrial soil (Yin et al., 2013, 2014). A recent study by Žárský et al. (2022) suggested the expansion of the first terrestrial flora during the Cryogenian interglacial period. Terrestrial materials during the E-C transition may have negative Δ199Hg values (Deng et al., 2022). During the E-C transition, rapid continental motion driven by the plate rearrangement from Rodinia to the Gondwana supercontinent led to rifting of continents associated with extensive terrestrial erosion. The Ediacaran Dengying Formation (dolomite) in the Maoshi and Zhijin sections (Fig. 6**A**) suggests that those two sections were located in shallow platform settings during the late Ediacaran. The unconformity between the late Ediacaran Dengying Formation (dolomite) and the overlying Early Cambrian Niutitang Formation (black shale) in the Maoshi and Zhijin sections (Fig. 6**B**) suggests that the two sections rifted to above seawater levels and underwent terrestrial erosion during the E-C transition. In the Sansui section, the lack of an unconformity between the Ediacaran Liuchapo Formation (carbonaceous chert, equivalent to the Dengying Formation) and the Cambrian Jiumenchong Formation (black shale, equivalent to Niutitang Formation) suggests that this section was continuously located beneath the seawater level during the E-C transition (Feng et al., 2014, Chen et al., 2015). As a result, the Sansui area would have received a substantial amount of terrestrial material due to nearby terrestrial erosion. This is supported by the paleogeographic location near the Jiangnan paleo-islands (Fig. 1**B**).

In the Early Cambrian, Δ^{199}Hg of the black shales in the Sansui section shifted from −0.03 ‰ to positive values up to 0.18 ‰, especially in the V shale unit (Fig. 6**C**). The latter value is a distinct marine signal, consistent with the composition of modern seawater, and suggests that Hg was mainly sourced from the global marine seawater reservoir, with little or no contribution from near-shore, i.e. riverine sources. Positive Δ^{199}Hg values were observed in the Early Cambrian polymetallic Ni-Mo-rich sulfidic black shales (0.10–0.22‰) and phosphorites (0.13–0.24‰) from the Maoshi and Zhijin sections, respectively, in which Hg was derived from seawater via the organic matter shuttle and sulfide fixation, given that organic matter has a strong affinity to seawater Hg (Yin et al. 2017). The positive correlation between Δ^{199}Hg and TOC in the Early Cambrian samples suggests that Hg was deposited mainly via the organic matter shuttle (Fig. 7). As shown in Fig. 6**C**, we propose that during the Early Cambrian, the rifted continental margin of the Yangtze platform produced segmented carbonate uplifts which separated the transitional zone from the deep basin to form a restricted offshore basin environment in the transitional zone. Such an environment, associated with rising seawater levels, i.e. transgression, and strong terrestrial erosion (as expected from the topographic relief created by rifting of the continental margin) contributed abundant nutrients to the restricted basin. This, in turn, resulted in high oceanic productivity and enhanced organic matter burial on the seafloor. The rain of organic matter produced anoxic/euxinic conditions in the lower part of the seawater column where incomplete organic matter decay and sulfate-reducing bacteria caused black shale and sulfide deposition (Johnson et al., 2017; Frei et al., 2021; Lehmann et al., 2022). The anoxic/euxinic conditions in the deeper water column favored the deposition of seawater Hg and other metals (e.g., Mo-V-U), given their affinity to organic matter and/or reduced sulfur.

6. Conclusion

We observed a large variation of Δ^{199}Hg values in E-C samples in the Sansui section, which indicates changes in Hg sources as a function of near-coastal versus restricted basin setting in South China. The near-zero Δ^{199}Hg values in Late Ediacaran carbonaceous chert imply large input of

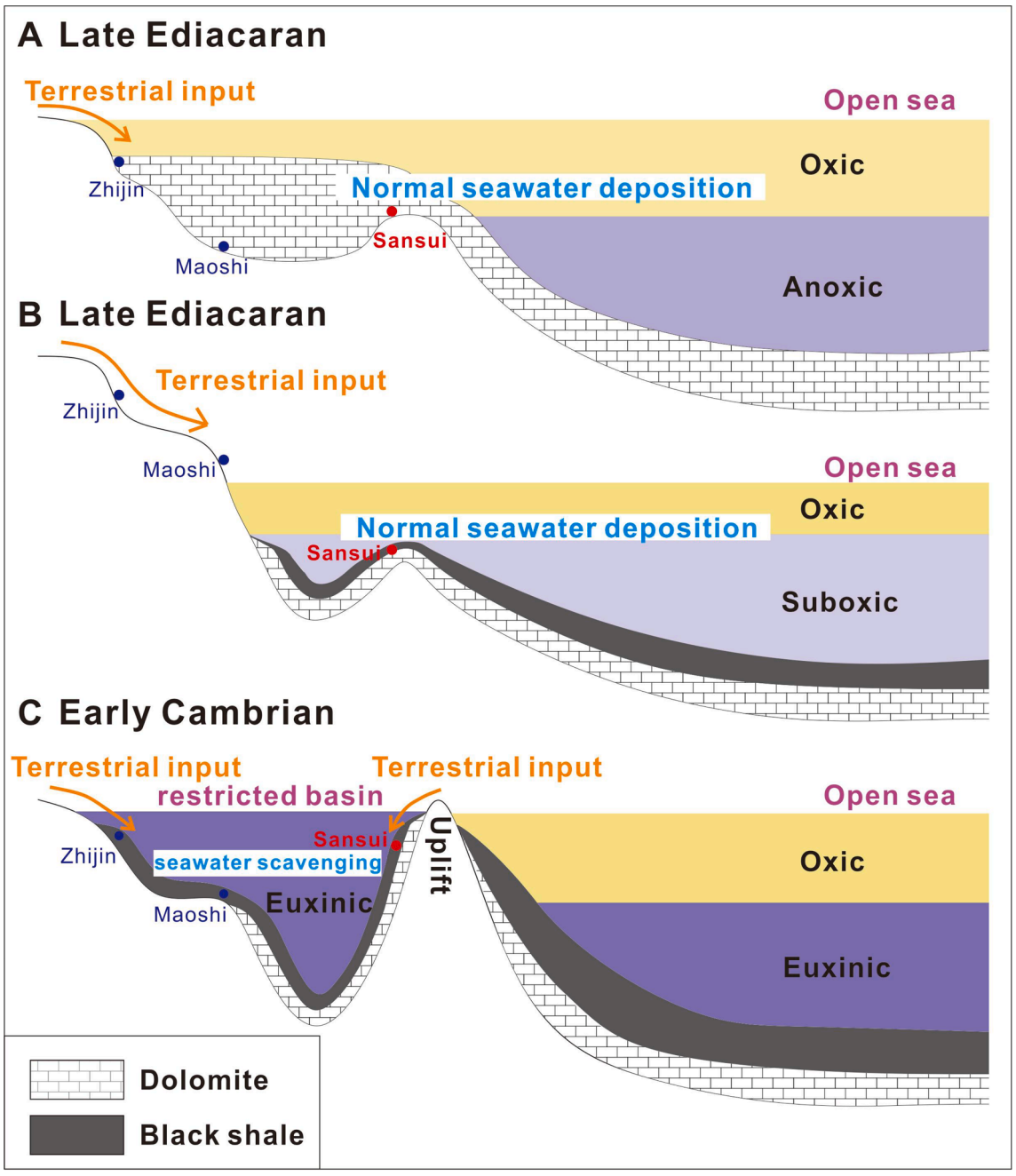

Fig. 6. A conceptual model showing the paleo-depositional setting and Hg sources to the ocean in South China, during (A-B) the Late Ediacaran and (C) the Early Cambrian.

terrestrial Hg (with negative Δ^{199}Hg values) or volcanic Hg (with near-zero Δ^{199}Hg values) in a transgressive near-coastal setting. The shift to positive Δ^{199}Hg values in the Early Cambrian metalliferous black shales with elevated Hg content suggests Hg was derived from the global seawater reservoir, and efficiently scavenged in a restricted basin setting with very low clastic input. Our study is in line with a model of regional ocean dynamics in the Early Cambrian, with the interplay of terrestrial and global marine reservoirs in the control of oceanic productivity, seawater redox conditions and the deposition of metalliferous shales, as also shown by other stable isotope systems, such as Cr and Cd (Lehmann et al., 2016; Frei et al., 2020, 2021).

CRediT authorship contribution statement

Zhongxi Xue: Investigation, Writing – original draft. **Runsheng Yin:** Conceptualization, Methodology, Supervision, Writing – original draft. **Bernd Lehmann:** Supervision, Writing – original draft. **Ruidong Yang:** Conceptualization, Methodology, Supervision. **Hai Xu:** Data curation, Investigation. **Jun Chen:** Data curation, Investigation. **Hongyan Geng:** Data curation, Investigation. **Junbo Gao:** Conceptualization, Methodology, Supervision, Writing – original draft.

Declaration of Competing Interest

The authors declare that they have no known competing financial interests or personal relationships that could have appeared to influence

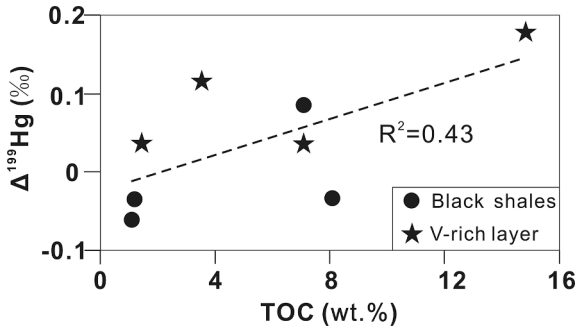

Fig. 7. Correlation diagram of Δ^{199}Hg and TOC for the Sansui section samples from the Early Cambrian Jiumenchong Formation.

the work reported in this paper.

Acknowledgements

This paper was supported by the National Natural Science Foundation of China (No: 42163006, 41890841), Talent Base Project in Guizhou Province (No: RCJD2018-21), Cultivation Project of Guizhou University (No: 202007), and the Guizhou Province Graduate Research Fund Project (No: YJSCXJH[2020]181).

Appendix A. Supplementary material

Supplementary data to this article can be found online at https://doi.org/10.1016/j.precamres.2022.106749.

References

Algeo, T.J., Lyons, T.W., 2006. Mo–total organic carbon covariation in modern anoxic marine environments: Implications for analysis of paleoredox and paleohydrographic conditions. Paleoceanography 21 (1), n/a–n/a.
Algeo, T.J., Tribovillard, N., 2009. Environmental analysis of paleoceanographic systems based on molybdenum–uranium covariation. Chem. Geol. 268 (3-4), 211–225.
Blum, J.D., Bergquist, B.A., 2007. Reporting of variations in the natural isotopic composition of mercury. Anal. Bioanal. Chem. 388 (2), 353–359.
Blum, J.D., Sherman, L.S., Johnson, M.W., 2014. Mercury isotopes in earth and environmental sciences. Annu. Rev. Earth Planet. Sci. 42 (1), 249–269.
Chen, D., Zhou, X., Fu, Y., Wang, J., Yan, D., 2015. New U-Pb zircon ages of the Ediacaran-Cambrian boundary strata in South China. Terra Nova 27 (1), 62–68.
Coveney Jr., R.M., Grauch, R.I., Murowchick, J.B., 1994. Metals, phosphate and stone coal in the Proterozoic and Cambrian of China: the geologic setting of precious metal–bearing Ni–Mo ore beds. Soc. Econ. Geol. Newslett. 18, 1–11.
Darroch, S.A.F., Smith, E.F., Laflamme, M., Erwin, D.H., 2018. Ediacaran extinction and Cambrian explosion. Trends Ecol. Evol. 33 (9), 653–663.
Deng, C., Geng, H., Xiao, T., Chen, D.i., Sun, G., Yin, R., 2022. Mercury isotopic compositions of the Precambrian rocks and implications for tracing mercury cycling in Earth's interior. Precambr. Res. 373, 106646.
Fan, H.F., Wen, H.J., Han, T., Zhu, X.K., Feng, L.J., Chang, H.J., 2018. Oceanic redox condition during the late Ediacaran (551–541 Ma), South China. Geochim. Cosmochim. Acta 238, 343–356.
Feng, L.J., Li, C., Huang, J., Chang, H.J., Chu, X.L., 2014. A sulfate control on marine mid-depth euxinia on the early Cambrian (ca. 529–521Ma) Yangtze platform, South China. Precambrian Res. 246, 123–133.
Frei, R., Lehmann, B., Xu, L., Frederiksen, J.A., 2020. Surface water oxygenation and bioproductivity – A link provided by combined chromium and cadmium isotopes in Early Cambrian metalliferous black shales (Nanhua Basin, South China). Chem. Geol. 552, 119785.
Frei, R., Xu, L., Frederiksen, J.A., Lehmann, B., 2021. Signals of combined chromium–cadmium isotopes in basin waters of the Early Cambrian – Results from the Maoshi and Zhijin sections, Yangtze Platform, South China. Chem. Geol. 563, 120061.
Grasby, S.E., Them, T.R., Chen, Z., Yin, R., Ardakani, O.H., 2019. Mercury as a proxy for volcanic emissions in the geologic record. Earth-Sci. Rev. 196, 102880.
Han, T., Zhu, X.Q., Li, K., Jiang, L., Zhao, C.H., Wang, Z.G., 2015. Metal sources for the polymetallic Ni–Mo–PGE mineralization in the black shales of the Lower Cambrian Niutitang Formation, South China. Ore Geol. Rev. 67, 158–169.
Han, T., Fan, H.F., Zhu, X.Q., Wen, H.J., Zhao, C.H., Fang, X., 2017. Submarine hydrothermal contribution for the extreme element accumulation during the early Cambrian, South China. Ore Geol. Rev. 86, 297–308.
Han, T., Fan, H.F., Wen, H.J., 2018. Dwindling vanadium in seawater during the early Cambrian, South China. Chem. Geol. 492, 20–29.
Jiang, S.-Y., Chen, Y.-Q., Ling, H.-F., Yang, J.-H., Feng, H.-Z., Ni, P., 2006. Trace– and rare– earth element geochemistry and Pb–Pb dating of black shales and intercalated Ni–Mo–PGE–Au sulfide ores in Lower Cambrian strata, Yangtze platform, South China. Mineral. Deposita 41 (5), 453–467.
Johnson, S.C., Large, R.R., Coveney, R.M., Kelley, K.D., Slack, J.F., Steadman, J.A., Gregory, D.D., Sack, P.J., Meffre, S., 2017. Secular distribution of highly metalliferous black shales corresponds with peaks in past atmosphere oxygenation. Miner. Deposita 52 (6), 791–798.
Ketris, M.P., Yudovich, Y.E., 2009. Estimations of Clarkes for carbonaceous biolithes: World averages for trace element contents in black shales and coals. Int. J. Coal Geol. 78 (2), 135–148.
Kirschvink, J.L., Ripperdan, R.L., Evans, D.A., 1997. Evidence for a large-scale reorganization of Early Cambrian continental masses by inertial interchange true polar wander. Science 277 (5325), 541–545.
Kwon, S.Y., Blum, J.D., Yin, R., Tsui, M.-K., Yang, Y.H., Choi, J.W., 2020. Mercury stable isotopes for monitoring the effectiveness of the Minamata Convention on Mercury. Earth Sci. Rev. 203, 103111.
Lehmann, B., Nägler, T.F., Holland, H.D., Wille, M., Mao, J.W., Pan, J.Y., Ma, D.S., Dulski, P., 2007. Highly metalliferous carbonaceous shale and Early Cambrian seawater. Geology 35, 403–406.
Lehmann, B., Frei, R., Xu, L., Mao, J., 2016. Early Cambrian black shale-hosted Mo-Ni and V mineralization on the rifted margin of the Yangtze platform, China: reconnaissance chromium isotope data and a refined metallogenic model. Econ. Geol. 111 (1), 89–103.
Lehmann, B., Pašava, J., Šebek, O., Andronikov, A., Frei, R., Xu, L.G., Mao, J.W., 2022. Early Cambrian highly metalliferous black shale in South China: Cu and Zn isotopes and a short review of other non-traditional stable isotopes. Miner. Deposita 1–12.
Li, C., Love, G.D., Lyons, T.W., Fike, D.A., Sessions, A.L., Chu, X., 2010. A stratified redox model for the Ediacaran ocean. Science 328 (5974), 80–83.
Li, C., Jin, C.S., Planavsky, N.J., Algeo, T.J., Cheng, M., Yang, X.L., Zhao, Y.L., Xie, S.C., 2017. Coupled oceanic oxygenation and metazoan diversification during the early–middle Cambrian? Geology 45, 743–746.
Lott, D.A., Coveney Jr., R.M., Murowchick, J.B., Grauch, R.I., 1999. Sedimentary exhalative nickel–molybdenum ores in South China. Econ. Geol. 94, 1051–1066.
Mao, J., Lehmann, B., Du, A., Zhang, G., Ma, D., Wang, Y., Zeng, M., Kerrich, R., 2002. Re-Os dating of polymetallic Ni–Mo–PGE–Au mineralization in lower Cambrian black shales of south China and its geologic significance. Econ. Geol. 97 (5), 1051–1061.
McLennan, S.M., 2001. Relationships between the trace element composition of sedimentary rocks and upper continental crust. Geochem. Geophys. Geosyst. 2 (4), n/a–n/a.
Merdith, A.S., Williams, S.E., Collins, A.S., Tetley, M.G., Mulder, J.A., Blades, M.L., Young, A., Armistead, S.E., Cannon, J., Zahirovic, S., Müller, R.D., 2021. Extending full–plate tectonic models into deep time: Linking the Neoproterozoic and the Phanerozoic. Earth Sci. Rev. 214, 103477.
Mitchell, R.N., Raub, T.D., Silva, S.C., Kirschvink, J.L., 2015. Was the Cambrian Explosion both an effect and an artifact of true polar wander? Am. J. Sci. 315 (10), 945–957.
Moynier, F., Jackson, M.G., Zhang, K., Cai, H.M., Halldórsson, S.A., Pik, R., Day, J.M.D., Chen, J.B., 2021. The Mercury Isotopic Composition of Earth's Mantle and the Use of Mass Independently Fractionated Hg to Test for Recycled Crust. Geophys. Res. Lett. 48 e2021GL094301.
Qin, Z., Xu, D.T., Kendall, B., Zhang, X.L., Ou, Q., Wang, X.Q., Li, J., Liu, J.G., 2022. Molybdenum isotope-based redox deviation driven by continental margin euxinia during the early Cambrian. Geochim. Cosmochim. Acta 325, 152–169.
Rudnick, R.L., Gao, S., 2003. Composition of the Continental Crust. In: Holland, H.D., TureKian, K.K., (Eds.), Treatise On Geochemistry, first ed. Pergamon, Oxford, vol. 3, pp. 1–64.
Selin, N.E., 2009. Global biogeochemical cycling of mercury: a review. Annu. Rev. Environ. Resour. 34 (1), 43–63.
Steiner, M., Wallis, E., Erdtmann, B.-D., Zhao, Y., Yang, R., 2001. Submarine–hydrothermal exhalative ore layers in black shales from South China and associated fossils–insights into a Lower Cambrian facies and bio–evolution. Palaeogeogr. Palaeoclimatol. Palaeoecol. 169 (3-4), 165–191.
Tribovillard, N., Algeo, T.J., Lyons, T., Riboulleau, A., 2006. Trace metals as paleoredox and paleoproductivity proxies: an update. Chem. Geol. 232 (1-2), 12–32.
Tribovillard, N., Algeo, T.J., Baudin, F., Riboulleau, A., 2012. Analysis of marine environmental conditions based on molybdenum–uranium covariation–applications to Mesozoic paleoceanography. Chem. Geol. 324–325, 46–58.
Wallis, E., 2007. The Climatic and Environmental History of the South Chinese Yangtze Platform During the Neoproterozoic and Early Cambrian: Hydrothermally Active and Salinity Stratified Epicontinental Basins a Key for Understanding the "Cambrian Explosion"? (Ph.D. thesis) TU Berlinpp. 1–227 (in German with English abstract).
Wang, W., Zhou, M.Z., Chu, Z.Y., Xu, J.J., Li, C.F., Luo, T.Y., Guo, J.H., 2020. Constraints on the Ediacaran-Cambrian boundary in deep-water realm in South China: Evidence from zircon CA-ID-TIMS U-Pb ages from the topmost Liuchapo Formation. Sci. China Earth Sci. 63 (8), 1176–1187.
Wang, X.Q., Shi, X.Y., Jiang, G.Q., Zhang, W.H., 2012. New U-Pb age from the basal Niutitang formation in South China: implications for dischronous development and condensation of stratigraphic units across the Yangtze platform at the Ediacaran-Cambrian transition. J. Asian Earth Sci. 48, 1–8.
Wood, R., Liu, A.G., Bowyer, F., Wilby, P.R., Dunn, F.S., Kenchington, C.G., Cuthill, J.F. H., Mitchell, E.G., Penny, A., 2019. Integrated records of environmental change and evolution challenge the Cambrian Explosion. Nat. Ecol. Evol. 3 (4), 528–538.

Wu, T., Yang, R.D., Gao, J.B., Li, J., 2021. Age of the lower Cambrian Vanadium deposit, East Guizhou, South China: Evidences from age of tuff and carbon isotope analysis along the Bagong section. Open Geosci. 13, 999–1012.
Xu, L.G., Lehmann, B., Mao, J.W., Qu, W.J., Du, A.D., 2011. Re–Os age of polymetallic Ni–Mo–PGE–Au mineralization in Early Cambrian black shales of South China–a reassessment. Econ. Geol. 106 (3), 511–522.
Xu, L.G., Lehmann, B., Mao, J.W., 2013. Seawater contribution to polymetallic Ni–Mo–PGE–Au mineralization in Early Cambrian black shales of South China: evidence from Mo isotope, PGE, trace element, and REE geochemistry. Ore Geol. Rev. 52, 66–84.
Xu, L., Mao, J., 2021. Trace element and C-S–Fe geochemistry of Early Cambrian black shales and associated polymetallic Ni–Mo sulfide and vanadium mineralization, South China: Implications for paleoceanic redox variation. Ore Geol. Rev. 135, 104210.
Yin, R., Feng, X., Meng, B., 2013. Stable mercury isotope variation in rice plants (Oryza sativa L.) from the Wanshan mercury mining district, SW China. Environ. Sci. Technol. 47 (5), 2238–2245.
Yin, R., Feng, X., Li, X., Yu, B., Du, B., 2014. Trends and advances in mercury stable isotopes as a geochemical tracer. Trends Environ. Anal. Chem. 2, 1–10.
Yin, R., Krabbenhoft, D.P., Bergquist, B.A., Zheng, W., Lepak, R.F., Hurley, J.P., 2016. Effects of mercury and thallium concentrations on high precision determination of mercury isotopic composition by Neptune Plus multiple collector inductively coupled plasma mass spectrometry. J. Anal. Atom. Spectrom. 31 (10), 2060–2068.
Yin, R.S., Xu, L.G., Lehmann, B., Lepak, R.F., Hurley, J.P., Mao, J.W., Feng, X.B., Hu, R. Z., 2017. Anomalous mercury enrichment in Early Cambrian black shales of South China: Mercury isotopes indicate a seawater source. Chem. Geol. 467, 159–167.
Yin, R., Chen, D.i., Pan, X., Deng, C., Chen, L., Song, X., Yu, S., Zhu, C., Wei, X., Xu, Y., Feng, X., Blum, J.D., Lehmann, B., 2022. Mantle Hg isotopic heterogeneity and evidence of oceanic Hg recycling into the mantle. Nat. Commun. 13 (1).
Žárský, J., Žárský, V., Hanáček, M., Žárský, V., 2022. Cryogenian glacial habitats as a plant terrestrialisation cradle–the origin of the anydrophytes and Zygnematophyceae split. Front. Plant Sci. 12, 735020.
Zambardi, T., Sonke, J.E., Toutain, J.P., Sortino, F., Shinohara, H., 2009. Mercury emissions and stable isotopic compositions at Vulcano Island (Italy). Earth Planet. Sci. Lett. 277 (1-2), 236–243.
Zerkle, A.L., Yin, R.S., Chen, C.Y., Li, X.D., Izon, G.J., Grasby, S.E., 2020. Anomalous fractionation of mercury isotopes in the Late Archean atmosphere. Nat. Commun. 11, 1709–1718.
Zhou, Z.B., Wen, H.J., Qin, C.J., Fourestier, J., Liu, L., Shi, Q.P., 2018. The genesis of the Dahebian Zn–Pb deposit and associated barite mineralization: implications for hydrothermal fluid venting events along the Nanhua Basin, South China. Ore Geol. Rev. 101, 785–802.
Zhu, G., Wang, P., Li, T., Zhao, K., Zheng, W., Feng, X., Shen, J., Grasby, S.E., Sun, G., Tang, S., Yan, H., 2021a. Mercury record of intense hydrothermal activity during the early Cambrian, South China. Palaeogeogr. Palaeoclimatol. Palaeoecol. 568, 110294.
Zhu, G., Zhao, K., Li, T., Zhang, Z., Tang, S., Wang, P., 2021b. Anomalously high enrichment of mercury in early Cambrian black shales in South China. J. Asian Earth Sci. 216, 104794.
Zhu, M., Zhang, J., Steiner, M., Yang, A., Li, G., Erdtmann, B., 2003. SinianCambrian stratigraphic framework for shallow- to deep-water environments of the Yangtze platform: an integrated approach. Prog. Nat. Sci. 13 (12), 951–960.